Single-Molecule Conductance

DOI: 10.1002/anie.201301665

Highly Conductive [3 × *n*] Gold-Ion Clusters Enclosed within Self-Assembled Cages**

Manabu Kiguchi, Junichi Inatomi, Yuuta Takahashi, Ryota Tanaka, Takafumi Osuga, Takashi Murase, Makoto Fujita,* Tomofumi Tada,* and Satoshi Watanabe**

There is an increasing interest in the electron conductivity of metal-atom wires at the single-molecule level because of their quantized electric properties applicable to conducting wires in ultra-small devices.[1–3] In contrast, the single-molecular conductivity of metal-ion wires has never been studied and whether the metal-ion wires are conductive or insulating has been a matter of debate,[4–6] because creating metal-ion arrays with a fixed cross section and length between nanogap electrodes is nontrivial. In recent years, several efficient methods have been developed for preparing multinuclear complexes with ordered metal-ion arrays. Among them, [3 × *n*] gold-ion clusters, enclosed in self-assembled cages **1** (Figure 1), are particularly interesting because the stacking number *n* is uniquely determined by the length of the pillar ligand (**4**). In expectation of efficient electron transport through metal-ion arrays, single-molecular electron conductivity through [3 × *n*] stacks of gold-ion clusters $(\mathbf{2})_n$ ($n = 1$, 2, or 3) was measured. The cages, **1**, which keep the metal ions highly ordered in a [3 × *n*] manner within the cavity, are excellent frameworks for accommodating π-stacked molecules and evaluating their electron-transport properties.[7,8] We show that the metal-ion arrays are highly conductive, the electron transport being comparable to that through metal-atom wires and the absolute conductance value being much larger than that of metal-linked organic wires.

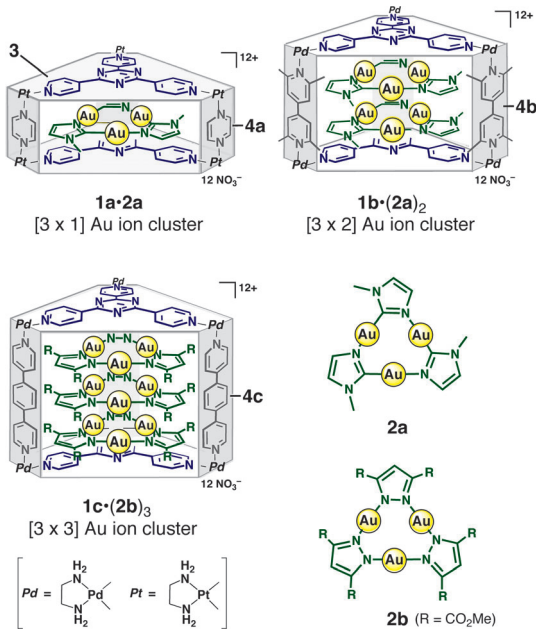

Figure 1. [3×*n*] Au^I ion clusters $(\mathbf{2})_n$ enclosed within coordination cages **1** which self-assemble from triazine panel ligands **3**, pillar ligand **4**, and [(ethylenediamine)M$(ONO_2)_2$] (M = Pd or Pt).

We confirmed by ab initio transport calculations that the [3 × *n*] Au^I ion clusters would be suitable for high conductance with a negligibly small decay over longer transport distances. We calculated the conductance of the corresponding model arrays, $\mathbf{3}\cdot(\mathbf{2a})_n\cdot\mathbf{3}$ ($n = 1$–4) (See the Supporting Information). Figure 2 shows the calculated conductance values, together

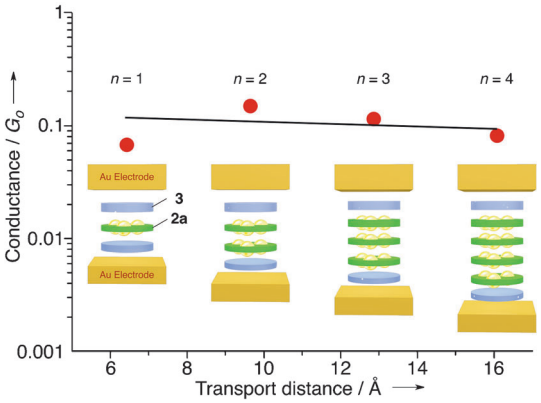

Figure 2. Computed conductance of [3 × *n*] Au^I ion clusters. In the calculation, the stacked arrays $\mathbf{3}\cdot(\mathbf{2a})_n\cdot\mathbf{3}$ ($n = 1$–4) sandwiched between Au electrodes were used as simple models for the [3 × *n*] Au^I ion clusters. The transport direction is parallel to the Au[111] direction.

[*] Dr. M. Kiguchi, J. Inatomi, Y. Takahashi
Department of Chemistry, Graduate School of Science and Engineering, Tokyo Institute of Technology
2-12-1 W4-10 Ookayama, Meguro-ku, Tokyo 152-8551 (Japan)
E-mail: kiguti.m.aa@m.titech.ac.jp

R. Tanaka, T. Osuga, Dr. T. Murase, Prof. Dr. M. Fujita
Department of Applied Chemistry, School of Engineering
The University of Tokyo
7-3-1 Hongo, Bunkyo-ku, Tokyo 113-8656 (Japan)
E-mail: mfujita@appchem.t.u-tokyo.ac.jp

Dr. T. Tada,[+] Prof. Dr. S. Watanabe
Department of Materials Engineering, School of Engineering
The University of Tokyo
7-3-1 Hongo, Bunkyo-ku, Tokyo 113-8656 (Japan)
E-mail: tada@cello.t.u-tokyo.ac.jp
watanabe@cello.t.u-tokyo.ac.jp

[+] Present address: Materials Research Center for Element Strategy
Tokyo Institute of Technology
4259-S2-13 Nagatsuta-cho, Midori-ku, Yokohama 226-8503 (Japan)

[**] This work was supported by JSPS KAKENHI Grant Numbers 23111706, 22104007, 20111007, 24000009.

Supporting information for this article is available on the WWW under http://dx.doi.org/10.1002/anie.201301665.

with the junction models. The high conductance values of approximately $0.1\,G_0\,(2e^2/h)$ were obtained regardless of the transport distance L. Fitting the data with the exponential decay of conductance [Eq. (1)]

$$G = A_N \exp(-\beta L) \qquad (1)$$

we obtained a reasonably small attenuation factor β of 0.02 Å^{-1}. Therefore, the $[3\times n]$ Au^{I} ion clusters in the nanogap are expected to be quite useful for high conducting wires with a large absolute conductance value and a small attenuation factor.

We measured the conductance of single $[3\times n]$ Au^{I} ion clusters trapped in the Au nanogap by the scanning tunneling microscope (STM) break junction technique (See the Supporting Information; Figure 3a).[9] The single $[3\times n]$ Au^{I} ion clusters are trapped in the Au nanogap, when the Au STM tip is repeatedly moved into and out of contact with an Au substrate in a solution containing the sample molecule. The conductance traces obtained from Au contacts in a solution of $[3\times 1]$ Au^{I} ion clusters are shown in Figure 3b. A sequence of steps appeared at integer multiples of $7\times10^{-3}\,G_0$ arising from the formation of molecular junctions. The conductance histograms, constructed from 1000 conductance traces, also showed peaks at the corresponding conductance values (Figure 3c, Figure S1–S3). When a solution of empty cage **1b** was measured, no plateaus or peaks were observed in the conductance traces or histograms between $0.03–5\times10^{-5}\,G_0$ and the measured conductance behavior was quite similar to the blank aqueous solution. From repeated measurements, the conductance value of the molecular junctions of $[3\times1]$ Au^{I} ion clusters was determined to be $7.0\pm1.6\times10^{-3}\,G_0$. We were able to directly measure the conductance of metal-ion arrays for the first time. From Figure 3d, we know that molecular junctions of $[3\times1]$ Au^{I} ion clusters formed immediately after breaking the Au atomic contact (Supporting Information, Figure S4). Statistical analysis of the single-molecule conductance traces provided evidence that the top and bottom panels of the $[3\times n]$ Au^{I} ion clusters bridged between the Au electrodes in the single-molecule junction (see Figure 3e and f, Figure S5). The maximum gap distance should be a good indicator of the true size of the molecule bridging the electrodes. For the $[3\times1]$ Au^{I} ion clusters, the obtained maximum gap distance of 0.6 nm was close to the intermolecular distance between the top and bottom panel ligands **3** (0.66 nm), indicating the bridging of the electrodes along the C_3 vertical axis of the cages (see the Supporting Information).

The conductances of single $[3\times2]$ and $[3\times3]$ Au^{I} ion clusters were measured and compared (Figure S1–S3). The conductance values of the molecular junctions of $[3\times2]$ and $[3\times3]$ Au^{I} ion clusters were determined to be $5.7\pm0.9\times10^{-3}\,G_0$ and $5.1\pm1.4\times10^{-3}\,G_0$, respectively. The temperature dependence measurement confirmed that electron transport through single $[3\times n]$ Au^{I} clusters occurred by a tunneling mechanism rather than a hopping mechanism. The conductance of the single $[3\times3]$ Au^{I} ion cluster did not depend on temperature in the temperature regime of 5–50 °C (Figure 4b, Figure S6).

The attenuation factor and contact resistance were evaluated based on the tunneling model. In this model, the conductance (G) of an atomic scale nanowire decays with the wire length, as described by Equation (1).[10] Where, A_N is the constant determined by the nanowire–electrode coupling strength and reflects the contact resistance; L is the length of the nanowire, and β is the exponential pre-factor that depends

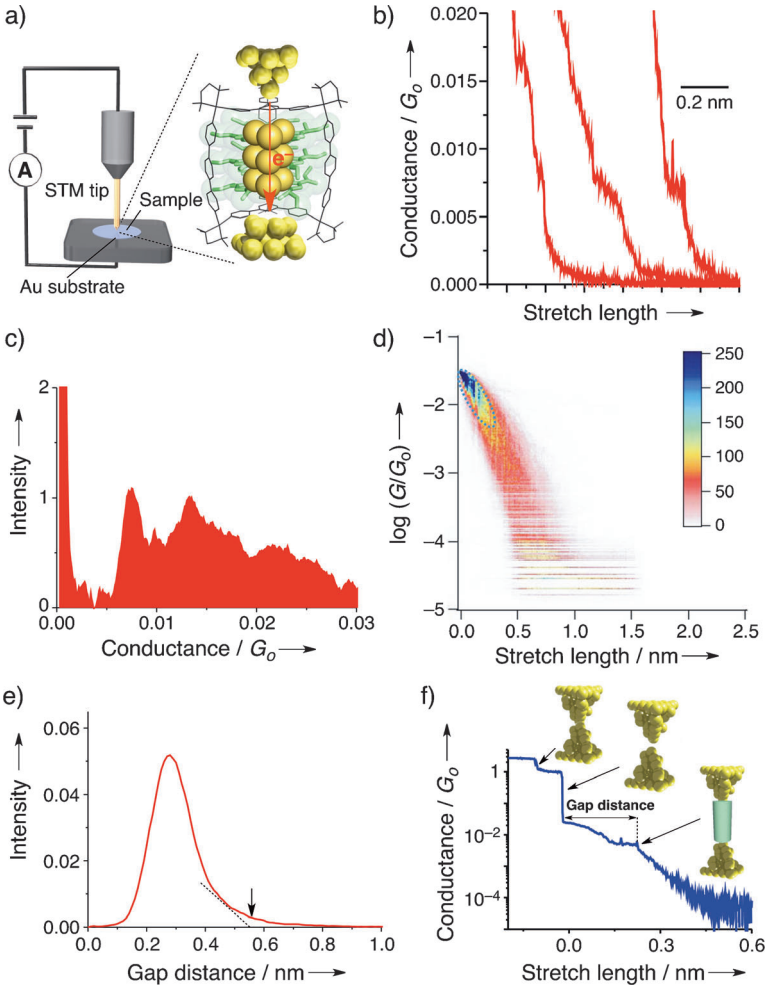

Figure 3. Conductance of $[3\times1]$ Au^{I} ion clusters. a) Schematic representation of the experimental setup for the single-molecule conductance measurement. The X-ray crystal structure of the $[3\times3]$ Au^{I} ion cluster is inserted into the schematic representation of the Au nanogap electrodes. b) Conductance curves of $[3\times1]$ Au^{I} ion clusters on a linear scale. c) Conductance histograms of $[3\times1]$ Au^{I} ion clusters showing steps. The tunneling background was subtracted (see the Supporting Information). d) Two-dimensional conductance histogram of the $[3\times1]$ Au^{I} ion clusters constructed from 2300 traces without data selection. The region with a large number of counts, encircled by the blue dashed lines, is visible. e) The distribution of gap distances of the $[3\times1]$ Au^{I} ion cluster junctions. The maximum gap distance is shown as an arrow. f) Example of a conductance curve, showing the data-point selection, together with a schematic junction formation mechanism.

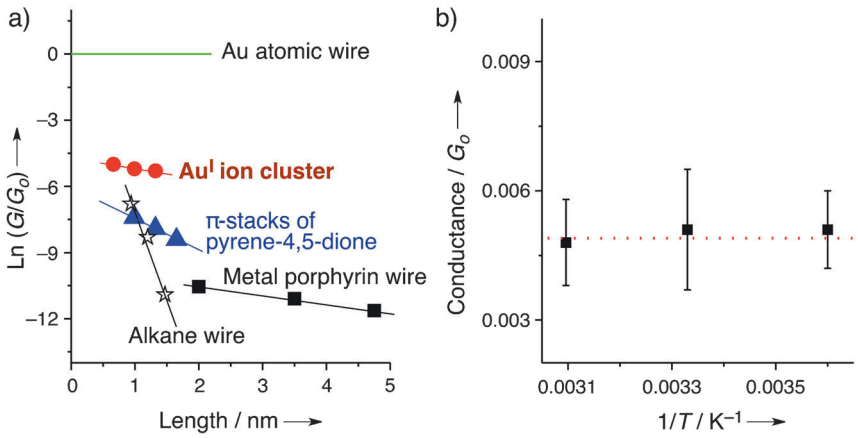

Figure 4. Conductance data for [3×*n*] Au^{I} ion cluster. a) Distance dependence of observed conductance *G* for the [3×*n*] Au^{I} ion clusters. Typical atomic scale nanowires (Au atomic wires, discrete π-stacks of pyrene-4,5-dione, metal porphyrin wires, and alkane wires) are also shown. b) Conductance of the single [3×3] Au^{I} ion cluster as a function of temperature.

on the electronic structure of the nanowire. Conductive nanowires have small β values whereas insulating nanowires have large values. The β value for the single [3×*n*] Au^{I} ion clusters was determined to be 0.05 Å^{-1} from the slope of *L* versus ln*G* plots (Figure 4a), which agrees with the theoretical prediction of small β values. The obtained β value is smaller than that of the vacuum gap ($\beta = 2.2$ Å^{-1}), organic alkanes ($\beta = 0.7 \approx 0.9$ Å^{-1}), and discrete π-stacks of pyrene-4,5-dione ($\beta = 0.1$ Å^{-1}), and comparable to that of porphyrin wires containing metal ions ($\beta = 0.04$ Å^{-1}).[7,11] The A_N value for the single [3×*n*] Au^{I} clusters was 1.1×10^{-2} G_0, which is larger than that of porphyrin wires containing metal ions ($A_N = 6 \times 10^{-5}$ G_0) and the π-stacked system of pyrene-4,5-dione ($A_N = 1.5 \times 10^{-3}$ G_0). Accordingly, we were able to directly fabricate single metal-ion arrays trapped between metal electrodes showing both a small attenuation factor and low contact resistance.

To determine the reasons for the high conductance in the discrete Au^{I} ion arrays, we further investigated the transmission functions and local density of states (LDOS) around the Fermi level from ab initio non-equilibrium Green's function calculations,[12–15] especially for the stack model (**3**)·(**2a**)$_2$·(**3**) geometry optimized with Gaussian 09[16] (see the Supporting Information). Figure 5 shows the calculated transmission function (Figure 5a), computational model (Figure 5a and b), and LDOS of (**3**)·(**2a**)$_2$·(**3**) (Figure 5c–f). The calculated LDOS at 0.1 eV below the Fermi level showed that the main electron pathway is composed of the d-orbitals of the Au$^{I}_6$ ion cluster in (**2a**)$_2$ (Figure 5c), which is supported by the π-orbitals of the panel **3** (Figure 5d). That is, the π-orbitals of the panel molecule and the d-orbitals of the Au^{I} ion arrays are well connected with the electrodes, leading to the high conductance region below the Fermi level. On the other hand, at 0.1 eV above the Fermi level, the electron pathway from the d-orbitals of the Au$^{I}_6$ ion cluster cannot be confirmed (Figure 5e), although the orbitals of the panel **3** are still ready to serve the electron pathway (Figure 5f). The transmission function therefore decreases dramatically above the Fermi level. The similar metallic channels below the Fermi level and the broken channels above the Fermi level were also confirmed in the other Au^{I} ion clusters (**3**)·(**2a**)·(**3**) and (**3**)·(**2b**)$_3$·(**3**). Therefore, the high-transmission region closely positioned below the Fermi level served by the Au^{I} ion arrays was found to be essential to hold the high conductance in the molecular junctions of the discrete Au^{I} ion arrays.

In conclusion, we succeeded in directly measuring electron transport through single discrete metal-ion arrays trapped in the Au nanogap, using [3×*n*] Au^{I} complexes, in which the number and relative position of Au^{I} ions are well defined within the cages. We demonstrate electron transport through metal-ion arrays with low attenuation which is comparable to that through meta-atom wires. In addition, the contact resistance

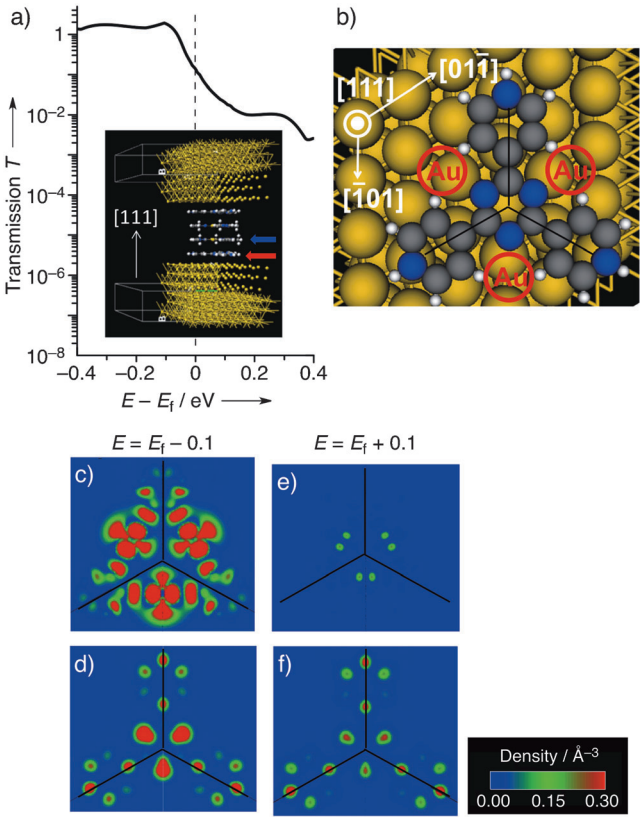

Figure 5. Calculated conductance of the [3×2] Au^{I} ion cluster. a) Calculated transmission function of the stacked model (**3**)·(**2a**)$_2$·(**3**). Inset: side view of the computational model. b) Top view of the model in which panel ligand **3** and the bottom electrodes are depicted (Au yellow, N blue, C gray, H white). The red circles with index Au indicate the position of the Au^{I} atoms in **2a** located above the panel ligand **3**. The black lines are introduced as the guide of the C_3 symmetry. c,d) the local density of states at 0.1 eV below the Fermi level on **2a** plane (the blue arrow of the inset of (a)) and panel ligand **3** plane (the red arrow of the inset of (a)), respectively. e,f) the local density of states at 0.1 eV above the Fermi level on **2a** and **3** planes, respectively.

is much smaller in the metal ion arrays than in other organic wires containing metal ions. These experimental and theoretical results may shed new light on the potential benefits of conductive wires using metal-ion arrays, and on the basic science of one-dimensional physics.

Received: February 26, 2013
Published online: April 29, 2013

Keywords: cluster compounds · electron transfer · gold · molecular electronics · single-molecule studies

[1] a) R. E. Peierls, *Quantum Theory of Solids*, Clarendon, Oxford, **1964**; b) J. M. Luttinger, *J. Math. Phys.* **1963**, *4*, 1154 – 1162.
[2] N. Agraït, A. L. Yeyati, J. M. van Ruitenbeek, *Phys. Rep.* **2003**, *377*, 81 – 279.
[3] H. Ohnishi, Y. Kondoh, K. Takayanagi, *Nature* **1998**, *395*, 780 – 783.
[4] N. Kamaya, K. Homma, Y. Yamakawa, M. Hirayama, R. Kanno, M. Yonemura, T. Kamiyama, Y. Kato, S. Hama, K. Kawamoto, A. Mitsui, *Nat. Mater.* **2011**, *10*, 682 – 686.
[5] T. B. Reddy, *Handbook of Batteries*, 4th ed., McGraw-Hill, New York, **2011**.
[6] B. Hille, *Ion Channels of Excitable Membranes*, Sinauer Associates, Sunderland, MA, **2001**.
[7] M. Kiguchi, T. Takahashi, Y. Takahashi, Y. Yamauchi, T. Murase, M. Fujita, T. Tada, S. Watanabe, *Angew. Chem.* **2011**, *123*, 5826 – 5829; *Angew. Chem. Int. Ed.* **2011**, *50*, 5708 – 5711.
[8] a) M. Yoshizawa, J. K. Klosterman, M. Fujita, *Angew. Chem.* **2009**, *121*, 3470 – 3490; *Angew. Chem. Int. Ed.* **2009**, *48*, 3418 – 3438; b) T. Osuga, T. Murase, K. Ono, Y. Yamauchi, M. Fujita, *J. Am. Chem. Soc.* **2010**, *132*, 15553 – 15555; c) T. Osuga, T. Murase, M. Fujita, *Angew. Chem.* **2012**, *124*, 12365 – 12367; *Angew. Chem. Int. Ed.* **2012**, *51*, 12199 – 12201.
[9] a) N. J. Tao, *Nat. Nanotechnol.* **2006**, *1*, 173 – 181; b) A. Mishchenko, L. A. Zotti, D. Vonlanthen, M. Burkle, F. Pauly, J. C. Cuevas, M. Mayor, T. Wandlowski, *J. Am. Chem. Soc.* **2011**, *133*, 184 – 187.
[10] a) X. Li, J. He, J. Hihath, B. Xu, S. M. Lindsay, N. Tao, *J. Am. Chem. Soc.* **2006**, *128*, 2135 – 2141; b) X. Xiao, B. Xu, N. Tao, *J. Am. Chem. Soc.* **2004**, *126*, 5370 – 5371; c) G. Sedghi, K. Sawada, L. J. Esdaile, M. Hoffmann, H. L. Anderson, D. Bethell, W. Haiss, S. J. Higgins, R. J. Nichols, *J. Am. Chem. Soc.* **2008**, *130*, 8582 – 8583.
[11] a) F. Chen, X. Li, J. Hihath, Z. Huang, N. Tao, *J. Am. Chem. Soc.* **2006**, *128*, 15874 – 15881; b) G. Sedghi, V. M. García-Suárez, L. J. Esdaile, H. L. Anderson, C. J. Lambert, S. Martín, D. Bethell, S. J. Higgins, M. Elliott, N. Bennett, J. E. Macdonald, R. J. Nichols, *Nat. Nanotechnol.* **2011**, *6*, 517 – 523.
[12] S. Datta, *Electronic transport in mesoscopic systems*, Cambridge University Press, Cambridge, **1995**.
[13] M. Brandbyge, J.-K. Mozos, P. Ordejón, J. Taylor, K. Stokbro, *Phys. Rev. B* **2002**, *65*, 165401.
[14] ATK Manual "ATK version 11.8.1", QuantumWise A/S (http://www.quantumwise.com).
[15] J. P. Perdew, K. Burke, M. Ernzerhof, *Phys. Rev. Lett.* **1996**, *77*, 3865 – 3868.
[16] M. J. Frisch, et al. Gaussian 09, revision C.01, Gaussian, Inc., Wallingford CT, **2010**. See the Supporting Information for full reference.

